Computers in Biology and Medicine 107 (2019) 10–17

Contents lists available at ScienceDirect

Computers in Biology and Medicine

journal homepage: www.elsevier.com/locate/compbiomed

Proximal detection of guide wire perforation using feature extraction from bispectral audio signal analysis combined with machine learning

Naghmeh Mahmoodian*, Anna Schaufler, Ali Pashazadeh, Axel Boese, Michael Friebe, Alfredo Illanes

INKA Intelligente Katheter, Otto-von-Guericke-Universität, Magdeburg, Germany

ARTICLE INFO

Keywords:
Acoustic emission
Bispectral analysis
Guide wire perforation

ABSTRACT

Artery perforation during a vascular catheterization procedure is a potentially life threatening event. It is of particular importance for the surgeons to be aware of hidden or non-obvious events. To minimize the impact it is crucial for the surgeon to detect such a perforation very early. We propose a novel approach to identify perforations based on the acquisition and analysis of audio signals on the outside proximal end of a guide wire. The signals were acquired using a stethoscope equipped with a microphone and attached to the proximal end of the guide wire via a 3D printed adapter. Bispectral analysis was employed to extract acoustic signatures in the signal and several features were extracted from the bispectrum of the signal. Finally, three machine learning algorithms - K-nearest Neighbor, Support Vector Machine (SVM), and Artificial Neural Network (ANN)- were used to classify a signal as a perforation or as an artifact. The bispectrum-based features resulted in valuable features allowing a perforation to be clearly identifiable from other occurring events. A perforation leaves a clear audio signal trace in the time-frequency domain. The recordings were classified as perforation, friction or guide wire bump using SVM with 97% (polykernel) and 98.62% (RBF) accuracy, k-nearest Neighbor an accuracy of 98.28% and ANN with accuracy of 98.73% was obtained. The presented approach shows that interactions starting at the tip of a guide wire can be picked up at its proximal end providing a valuable additional information that could be used during a guide wire procedure.

1. Introduction

Perforation of the vessel walls during guide wire applications could be a serious risk to the patient. The rate of occurrence for the percutaneous coronary intervention has been reported in the range of 0.1% and 4.0% [1–3]. To minimize the impact it is crucial for the surgeon to detect such a perforation very early. In planar X-ray imaging the vasculature and the vessel walls cannot be seen and consequently a perforation is not always recognized or detected. Therefore, besides X-ray imaging, additional real time information to detect guide wire perforation is an unmet-medical need worth to be addressed.

Several approaches has been proposed for acquiring additional guidance information from guide wires using different type of sensors. Most of them are based on acquiring haptic information from force measurements using piezoresistive sensors and most of them are integrated in or on the tip of the device. In Refs. [4–7] a haptic assistive system was implemented that allows the surgeon to feel forces acting on the guide wire tip. A piezoresistive force sensor is used for measuring contact forces within the arteries in order to improve navigation of guide wires during interventions. In Ref. [8], a sensor for integration into a torque device was developed. This sensor measures the interaction forces at the user's fingertips. The information is used to adjust the strength of the feedback to the varying frictional forces along the wire and thus to stabilize the system. Han et al. [9] developed and characterized a tri-axial force sensor embedded in the tip of a guide wire consisting of a piezoresistive sensing element using silicon nanowires. This design allowed the measurement of both normal and shear forces on the guide wire tip. Ganet et al. [10] presents the modeling and development of a steerable guide wire with two degrees of freedom capable of sensing force thanks to the pseudo-piezoelectric behavior of a polymer exposed to a DC-biased electrical field.

Other works have proposed piezoelectric and optical sensors for measuring pressure [11,12] and piezoelectric transducers for measuring blood flow velocity for monitoring vessel occlusion [13,14]. In this context the integration of an ultrasound transducer and pressure sensor was proposed in Ref. [15] in order to measure blood pressure and velocity in coronary arteries and in Ref. [16] a proof-of-concept of extreme miniaturization to include intravascular ultrasound capabilities

* Corresponding author.
E-mail address: naghmeh.ma56@yahoo.com (N. Mahmoodian).

https://doi.org/10.1016/j.compbiomed.2019.02.001
Received 8 October 2018; Received in revised form 25 January 2019; Accepted 2 February 2019

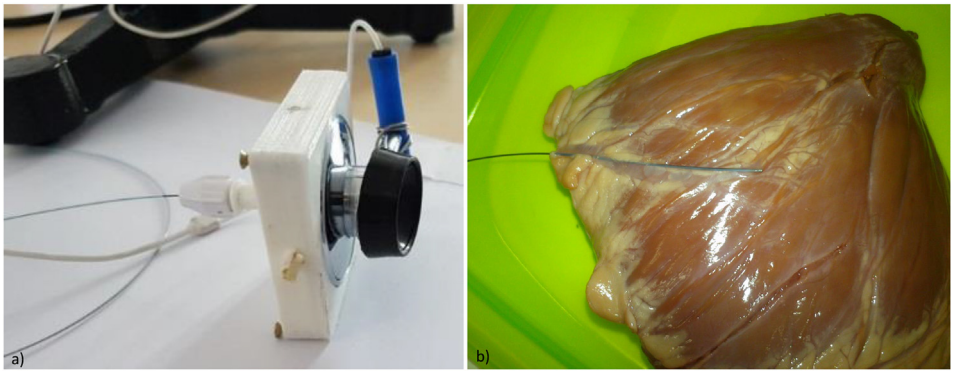

Fig. 1. a) view of the guide wire attached to a stethoscope connected to a microphone, b) guide wire inserted in a pork heart vessel [21].

on a guide wire was proposed. Another idea for measuring blood velocity was proposed in Refs. [17,18] through the use of temperature sensors and heating elements.

Another possible function that can be performed by the integration of sensors into the wire is the position tracking of the wire tip by installing one or more position sensors in the form of coils on the distal end of the wire [19,20].

While these methods could provide useful information to the surgeons during the clinical procedures, all of them suffer from a common drawback of increasing the complexity and costs of the guide wire. The sensors have to be embedded at the distal part of the guide wire that is inserted inside the body. Another important disadvantage of embedded sensors at the tip of a guide wire is the change of mechanical properties. Additional wires and sensors result in a reduction of the major functionality of being a *good guide wire* that is flexible, symmetric, trackable and traceable.

Additionally, even if some force sensor are placed at the proximal end of a guide wire, these systems are typically single-points sensing mechanisms or contact probes based on force feedback measurements. This means that only static information can be extracted while the movement of a guide wire through the arteries is dynamic.

A novel approach for acquiring additional signal information from medical interventional devices (MID), and specifically from a guide wire, has been recently proposed by our research group in Refs. [21,22]. In this works audio signals were acquired using a stethoscope connected to a microphone, which was attached to the proximal end of the MID via a 3D printed adapter and audio signals were recorded from the proximal end of the MID in order to extract information of the interaction between the distal tip and the tissue. The major advantage of this approach is that the system, audio receiver (stethoscope) and the sound box, are attached to the part of the guide wire that is outside the body. Thus, the setup can be used with conventional guide wires without changing the functionality of these devices to acquire audio signals. Additionally, unlike force feedback systems, audio sensing is a passive sensing technique involving dynamic information, fast reactions and high sensitivity to subtle changes in processes. The main idea of the proposed approach in the case of guide wire was to classify an event as being a vessel perforation or an artifact. Unlike the signal processing strategy proposed in Refs. [21,22], where a parametric approach was used, in this new work we propose a new classification approach based on features extracted from the audio signal using bispectral analysis. The main advantage of the proposed processing approach is that, unlike the parametrical approach, the bispectrum technique takes into account the non linearities and the phase relationships dynamics that this kind of complex signals can involve.

Results show that from the audio signal bispectrum it is possible to extract different features that are significant for being able to differentiate between vessel perforation and other events occurring during the guide wire insertion. Two classification methods using the extracting features obtained from more than 800 audio recordings show an accuracy higher than 95% for classifying a guide wire event as a perforation.

2. Materials and methods

The main idea of this work is to analyze and process audio recordings obtained from the interaction of the tip of the guide wire with the vessel wall using higher order statistics. This is done in order to find a nonlinear signature in the signal that allows to distinguish between a guide wire perforation and other events occurring during a guide wire insertion. For that the audio signals were processed and analyzed using bispectrum analysis and then 10 bispectrum based features were extracted and fed into two machine learning algorithms for classifying a guide wire event as a perforation or an artifact. In this section the experimental setup for obtaining a database of guide wire audio recordings is first presented. Then all the steps of the signal processing strategy based on bispectrum analysis are presented.

2.1. Experimental setup and database implementation

Audio signals were acquired using a stethoscope connected to a microphone which was directly and firmly attached to the proximal end of a 0.014-inch guide wire of 1.8 m length (Boston Scientific, US) placed inside a flushed 1.9 F micro catheter of 1.5 m length [22] (see Fig. 1).

Ten pork heart vessels were perforated by using the tip of the guide wire as explained in Ref. [22]. Subsequently 871 audio signals of 30 s duration were recorded in WAV format with a frequency sampling rate of 44100 HZ. The generated audio signal database contains 559 artery perforation and 312 non-perforation signals including manually generated artifacts as guide wire friction (214 recordings) and bumps (98 recordings).

2.2. Audio signal processing and classification

In this section the main steps of the signal processing approach used in this work for classifying an audio recording as guide wire perforation

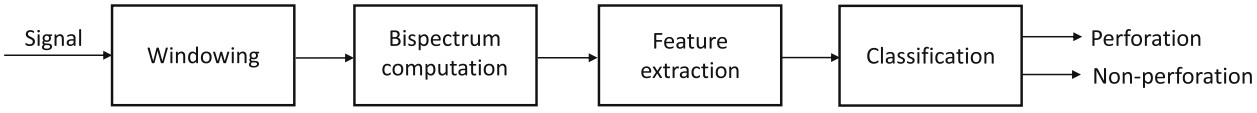

Fig. 2. Main steps for processing an audio signal recording for classifying it as perforation or artifact.

or artifact are presented. The main steps of the algorithm are shown in the scheme of Fig. 2. As a first step the signal was windowed in order to extract overlapped segments to track time-varying characteristics of the signal. The bispectrum was then computed for each signal segment from which 10 different features were extracted. From the time-Varying features a procedure is performed that classifies a recording as being a vessel perforation or an artifact. For that two known machine learning techniques were used.

2.2.1. Windowing

Due to the time-variant characteristics of the audio recordings a time varying bispectrum has to be computed through a sliding window. For that it is required to select two important parameters namely as window length or window size -number of time sample- and overlap.

The window length should be long enough to allow the measurement of important dynamical changes related to a guide wire event, but short enough to be able to perform a time-variant analysis without significant reduction of the bispectrum resolution. The experiments showed that a vessel perforation event concentrates nearly all of its energy in a time interval of less than 100 ms, therefore the window length should be set to a value of less than 100 ms. Following this analysis and after testing different perforation signals, the window length was set to 34 ms. In Fig. 3 a perforation audio signal example is displayed. Here you can see that the energy of the signal (bottom figure) concentrates in an interval of approximately 65 ms length. On the top of this figure two windows at different time instants are displayed and plotted. These allow to observe in both, time-domain and frequency-domain (using a simple spectrogram), that the 34 ms length window contains significant information in terms of dynamical changes that can be tracked for signal characterization.

The overlap is measured based on the percentages of window length that can be considered 0% to almost 100% respectively for non and almost full overlapped. This parameter affects the duration and optimization rate of bispectrum computation [23]. One very important characteristic of the acquired audio signal is that a perforation event involves extremely fast frequency changes at the beginning of the event [22]. The dominant frequency can abruptly change and therefore, in order to not miss such a dynamical change, highly overlapped windows are required for tracking the characteristics of the perforation. A compromise needs to be achieved between big overlapping and computation time of the algorithm. For that it was decided to set the overlap to 90%.

2.2.2. Bispectral analysis

Bispectral or third order spectral analysis is an advanced signal processing technique that falls into the category of higher order spectral methods. This technique has been widely used in bio-signal analysis mainly for EEG and ECG applications. In EEG it has been used for detecting and predicting epileptic episodes [24,25] and classifying EEG based sleep stages [26], while for ECG analysis bispectral features have been extracted in order to identify patients with major depression [27], classifying types of heart beats [28] and for detecting obstructive sleep apnea [29]. The bispectrum has also been applied for audio signal analysis in biomedical engineering for the diagnosis of Alzheimer disease [30,31], in machinery fault diagnosis [32] and in non-destructive testing [33].

In this work we want to exploit the characteristics of bispectral analysis to process signals resulting from nonlinear processes in order to extract bispectral features for classifying a guide wire event as a perforation.

One of the main advantages of bispectral analysis is that it allows the extraction of non-linear characteristics of a signal and it also can assess deviation of data from Gaussianity [34]. Sign als originated from biological and biomedical systems are signals well suited to be processed with this type of nonlinear method [35]. Another good advantage for our purposes is that it gives information about the phase of the signal.

In this work the bispectrum is estimated for each window segment resulting from the windowing step explained in Section 2.2.1 by using the Fourier Transform third order cumulants sequence [23]. In order to perform bispectrum analysis the windowed signal segment is first divided into series of sub-segments or epochs. Then the bispectrum of the interrelationship between two frequencies (f_1 and f_2) is computed for each epoch as follows: [23,30,31,35–38].

$$B(f_1, f_2) = E[X_i(f_1)X_i(f_2)X_i^*(f_1 + f_2))] \quad (1)$$

where, $x_i(f)$ is the Fourier Transform of the signal epoch i and $E[.]$ is the ensemble average operator. In this case, ensemble average of 8 sub-windows containing 256 samples ($2^8 = 256$) were calculated based on the Fourier Transform of the third order cumulant function. The result

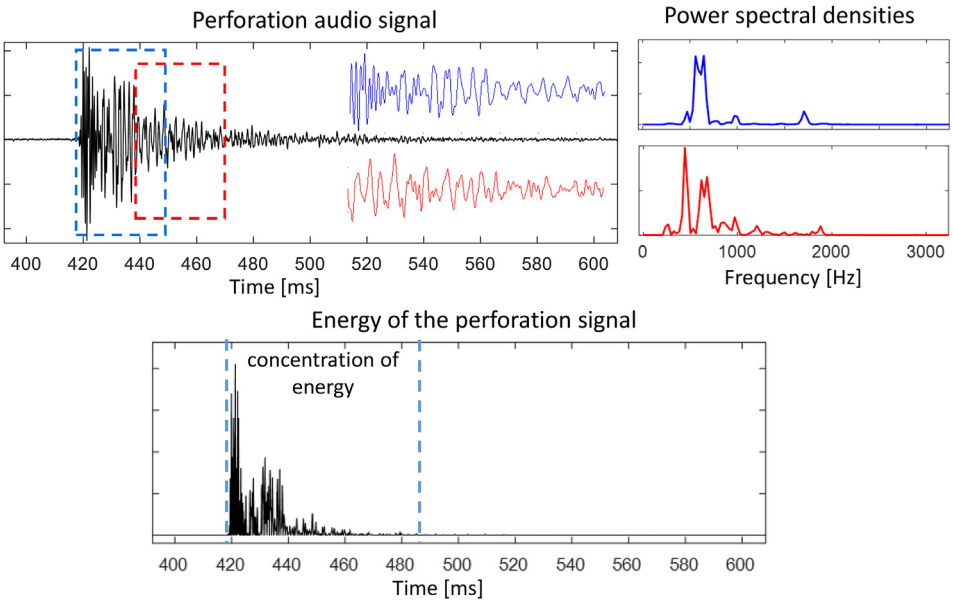

Fig. 3. Windowing step showing two windows during a guide wire event (time-domain and frequency-domain) and energy of the signal. The audio signal is segmented into sliding windows of 34 ms length with an overlap of 90%.

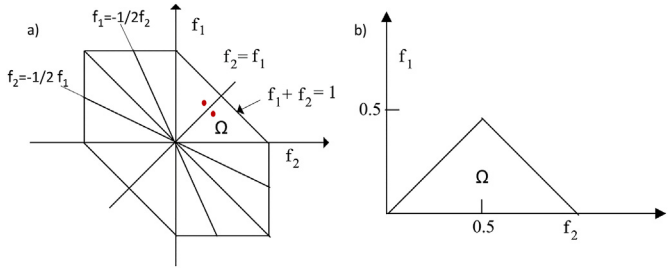

Fig. 4. a) Bispectrum area and b) Triangular region of the bispectrum [37].

leads to a 2D complex value bispectrum matrix with the size of 256 × 256 for each windowed segment of the audio recording signal. Finally, $X_i^*(f_1 + f_2)$ indicates the complex conjugate of $X_i(f_1 + f_2)$ at the frequencies f_1 and f_2.

The bispectrum B contains 12 areas where 6 are symmetric. Based on the location of the conjugate of equation (1) $w \in \{f_1 = f_2\}$ is used to estimate the bispectrum over $[0, \pi/2]$, which is the bispectrum part corresponding to the triangular region Ω [37] (see Fig. 4).

2.2.3. Feature extraction

Feature extraction is an important step in bispectrum analysis since the resulting bispectrum matrix computed from equation (1) for each window contains a large amounts of data. In this regard, the bispectrum values corresponding to the triangular area (Ω) are calculated under the conditions of $f_2 >= 0$, $f_1 >= f_2$ and $f_1 + f_2 <= 1$ [39,40].

In order to characterize the resulting audio signals from guide wire events, quantitative features must be extracted from the non-redundant region of the bispectrum matrix. Based on bispectral features already used in the literature [39,41–45], in this study 10 different bispectrum features are extracted. For each signal segment resulting from the windowing step a set of 10 features, linear and non-linear, computed directly from the triangular area Ω were extracted as follows:

1. Linear features corresponding to energy-based features computed as the mean (M_1), maximum (M_2) and minimum (M_3) of the bispectum energy, respectively:

$$M_1 = \frac{1}{m}\sum_{\Omega} |B(f_1, f_2)| \tag{2}$$

$$M_2 = \max|B(f_1, f_2)| \tag{3}$$

$$M_3 = \min|B(f_1, f_2)| \tag{4}$$

where m is the number of elements in the bispectrum region(Ω).

2. Non-linear features, which we have divided into two type of features. The first type corresponds to frequency-relation-based features involving the sum of the logarithmic amplitudes of the bispectrum S_1, the sum of the logarithmic amplitudes of the diagonal elements of the bispectrum S_2 and the first-order spectral moment of amplitudes of the diagonal elements of the bispectrum S_3. All these features are computed inside the bispectrum region Ω as [39,40]:

$$S_1 = \sum_{\Omega} \log(|B(f_1, f_2)|) \tag{5}$$

$$S_2 = \sum_{\Omega} \log(|B(f_k, f_k)|) \tag{6}$$

$$S_3 = \sum_{\Omega} K \log|B(f_1, f_2)| \tag{7}$$

The second type of nonlinear features involves bispectrum features based on the degree of data disorder or entropy. For that we compute the Phase entropy (pha) and the Entropy of phase of Domain E_j for j = 1,2,3 and also computed in the bispectrum area Ω [34,36,40]:

$$pha = \sum_{\Omega} |B(f_1, f_2)| \log\frac{1}{|B(f_1, f_2)|} \tag{8}$$

$$E_j = -\sum_{\Omega} \frac{|B(f_1, f_2)|^j}{\sum|B(f_1, f_2)|^j} \cdot \log\frac{\log|B(f_1, f_2)|^j}{\sum|B(f_1, f_2)|^j} \tag{9}$$

After the computation of the 10 features per window segment we computed the average of each feature over all the window segments as shown in Fig. 5 (n correspond to the total number of window segments resulting from the windowing step).

2.2.4. Classification

This section presents the classification algorithm used for classifying a guide wire event as a perforation or an artifact from the 10 bispectral features extracted as explained in the precedent section. For that we have tested three known machine learning algorithms, K-Nearest Neighbor (K-NN), Support Vector Machine (SVM), and ANN techniques, that will be introduced below.

2.2.4.1. Nearest neighbor classification. K-NN is one of the non-parametric classification methods and the simplest classifier with a comparative result. In this study the *Linear Nearest Neighbor* algorithm is chosen as an Instance-based algorithm for classification. Nearest Neighbor classifier assigns a new sample to the nearest training case based on similarity distance. Therefore, to classify and assign a new sample to a new class the distance of a sample was calculated using *M*inkowski distance algorithm. In K-NN algorithm K is the number of neighbors induced in the examination. This k value was set in 2 after the application of the Cross Validation method to select the best k value [46,47].

2.2.4.2. Support vector machine classification. In this work, SVM with *Polykernel* kernel with 10 features is used and it is defined as:

$$K(x, y) = (x^T y + c)^d$$

where T is used to train the SVM and later used for the classification

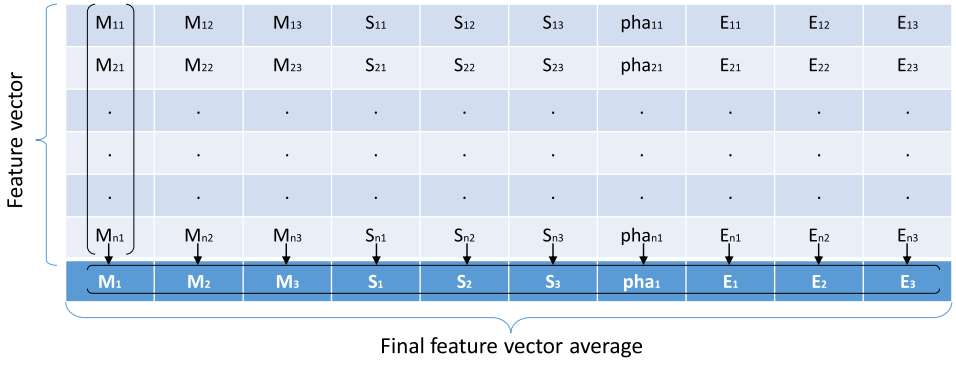

Fig. 5. Matrix showing the computation of the final 10 features per audio signal used for classification.

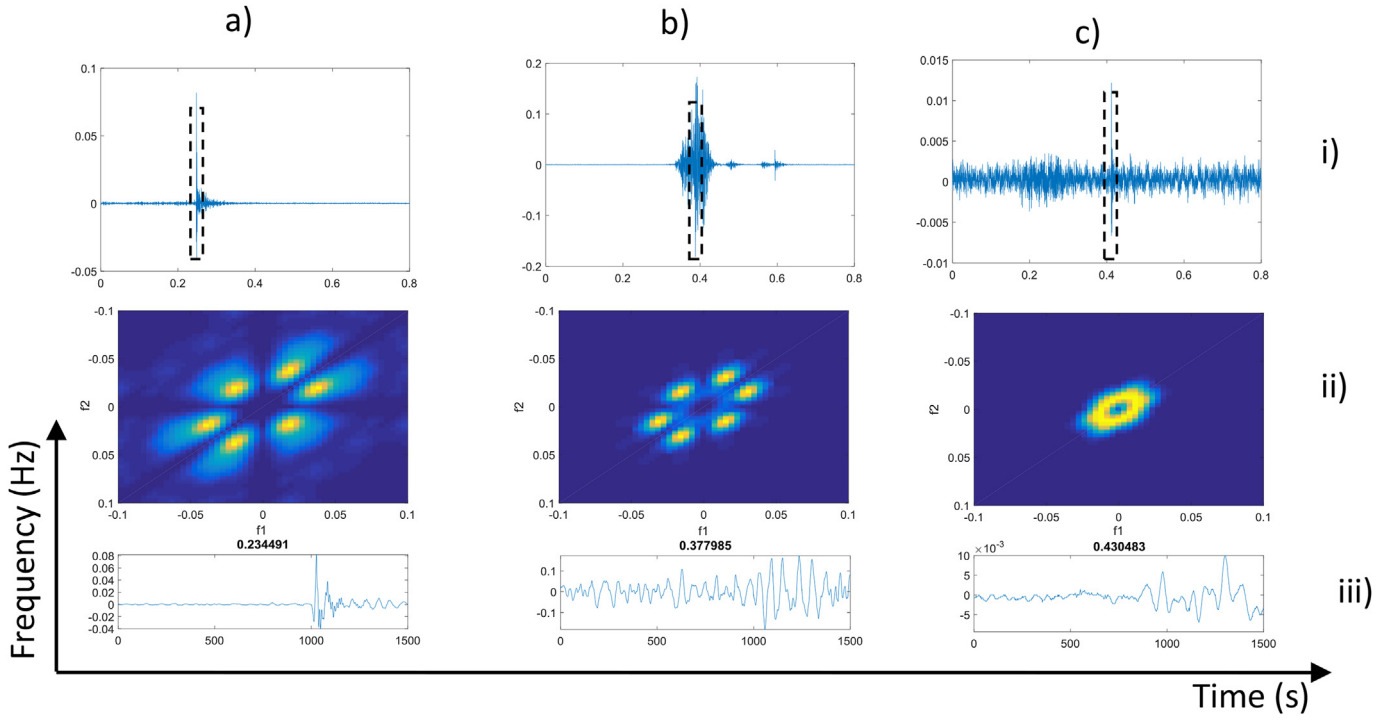

Fig. 6. (i) time domain raw audio signal (ii) bispectrum and (iii) windowed segment belonging to a) perforation, b)friction and c) bump.

task. The kernel x is an input vector, which in this study is ten-dimensional, y is the class label that in this case correspond to a multi-class, namely as perforation, friction and bump. $c >= 0$ is an hyper parameter, which is used as a trade-off to influence the higher-order versus lower-order terms in the polynomial. The exponent d of the function makes the kernel to be a polynomial and was set in this work as $d = 2$ in order to have a quadratic kernel [46,48].

Additionally, in order to classify non-linear separable data, SVM with a Gaussian kernel was employed. In this work Gaussian Radial Basis Function (RBF) was used as a transformation to transform feature space into higher order space. The RBF kernel is defined as:

$$K(x, y) = exp(-|x - y|^2/2\sigma^2) \quad (10)$$

Where σ is a scale parameter [49,50]. The grid search method was employed to optimize the parameter value of σ and the classification was carried out using a Sequential Minimal Optimization algorithm [51].

In this study in order to solve multi-class problem, a *pairwise* classifier trains a support vector machine to assign features into multi-class (perforation, friction and bump) [52]. We also use *Normalize training data* as a filtering parameter to normalize all features by default in order to reach an optimal model performance.

2.2.4.3. Artificial Neural Network. ANN is primarily an interconnected web of input nodes, hidden nodes and output nodes called artificial neurons. The classification using ANN was carried out using a multilayer perceptron with backpropagation training algorithm for classifying instances. The input layer consists of ten nodes which represent the features extracted from the bispectrum. The output layers consist of three nodes which represent perforation, friction and bump events. This network has up to 7 nodes in the hidden layers and a sigmoidal function was used for hidden nodes activation. The ten-fold cross validation method was employed for training and testing the data set. After several experiments, we found out that the process of training and optimizing the network have the best performance under the following condition: the networks were trained up to 500 epochs, learning rate of 0.2, momentum 0.2, and 3 layers. The selected network was applied in this study by employing WEKA 3.8.1 as a machine learning tool.

For all machine learning algorithm a 10-fold cross validation is used for training and testing data. In this technique a one-fold cross validation is used for testing and 9 for training. This is repeated 10 times and the final result is the average of 10 evaluations.

3. Results

Fig. 6 displays the main outcome of our approach. This figure presents three audio recordings for three different events occurring during a guide wire insertion: perforation, friction and bump (Fig. 6 a, b and c respectively). At the first row i) the time domain audio signal is displayed showing additionally a window segment located in the time interval where the event has occurred. In the second row ii) the bispectrum computed over the window segment is shown and in the third row iii) we show the time-domain signal of the windowed segments. If we observe the bispectrums of the three events it is evident that the dynamics of the signal during the event are completely different for a perforation, friction or a bump. This is the characteristic that we want to extract in order to be able to classify an event as being a perforation or an artifact.

Concerning the extracted features from the bispectrum the results show in general that when a perforation occurs some of the features present significant characteristic changes in their magnitude compared to a friction or a bump. In Fig. 7 we can observe the average value, computed over the 871 audio recordings of the database, of the three linear features (M_1, M_2 and M_3). As mentioned before, we can observe that the values of these three features are higher for guide wire perforation than for guide wire friction or bump.

In order to evaluate the differences in the bispectrum magnitudes, the 10 features were ranked using *Onerattribute* as an attribute emulator in order to show the features that have more impact on the classification accuracy (see Table 1). The results show that phase entropy has the highest rank while the minimum of the bispectrum domain has the lowest rank.

Fig. 8 displays 2D-scatters between the four best ranked features

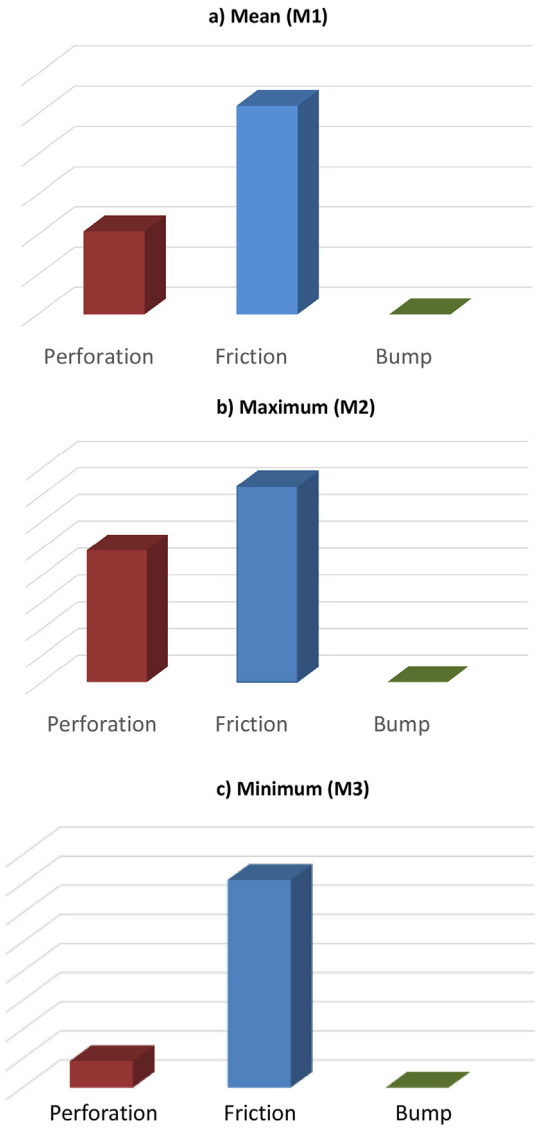

Fig. 7. Average magnitude of the linear features for guide wire perforation, friction and bump.

Table 1
Rank of linear and non-linear bespectrum-based features.

Rank Number	Rank Value	Features Name
1	89.4374	*pha*
2	88.4041	S_1
3	85.7635	S_2
4	85.6475	S_3
5	82.5488	M_1
6	77.9564	E_2
7	77.0379	M_2
8	75.4305	E_1
9	74.9713	E_3
10	70.9529	M_3

and the Fig. 9 shows a 3D scatter between three selected features. In both figures it is possible to visualize how the data can be separated in three clear clusters, belonging to each studied guide wire event. This confirms the significance of the bispectrum-based features for differentiating a perforation from other events and the unique bispectral characteristic that a perforation has compared to an artifact. These observations allow us to use methods as SVM and K-nearest neighbor for classifying an event as being perforation or artifact.

Machine learning techniques were employed to achieve specific information and to determine classification accuracy, sensitivity and specificity of the method. In order to evaluate these performance parameters, 2-NN and SVM algorithms were applied. False positive, accuracy, sensitivity and specificity are four primary performance measures of interest. The results of the four tested classification methods are presented in Table 2. It shows that 2-NN can classify the data with 0.010 false positive rate for perforation, 0.016 for friction and 0,001 for bump and 98.28% classification accuracy with 98% and 99% sensitivity and specificity respectively. Two SVM approaches (polykernel and RBF) were also used for classification of audio signals into three classes. It is possible to observe that the RBF-based SVM performs in general better than the polykernel-based one and similar than the 2-NN approach. Finally, results show that the A-NN approach present the best performances between the four tested algorithms. With an accuracy of 98.73% and a sensitivity and specificity of 99%, it outperforms the other classification procedures.

4. Discussions

As presented in the introduction section many solutions have been proposed in the literature for acquiring information from guide wires using different type of sensors, most of them embedded in the tip or located next to it, and few of them at the proximal end of the guide wire (outside the body). In terms of functionality if we compare the proposed audio approach with most of the literature results we can say that sensors located in or next to the tip result in direct contact of these sensors with human organs inside the body. This imposes serious design limitations for fulfilling clinical requirements. The most significant limitations are size-constraints and sterilization. For avoiding sterilization, the sensing device should be inexpensive enough for being a disposable device. Moreover, the sensor should be well-packaged for dealing with body liquids, and also, to protect the patient from any undesirable interaction with the tactile sensor itself. In summary these approaches have encounter difficulties to be inserted for regular clinical use because the direct integration requires to deal with certification issues, sterilization problems, additional cables, and significant increase in instrument cost. Unlike the prior works our proposed audio approach has several advantages that could allow a better integration for clinical use. The relative low cost, ease of integration and manufacturing could allow the development of add-on or completely new devices to acquire audio information in standard clinical devices and in standard clinical settings. A sort of plug-and-play device without the necessity of rebuild specialized instruments and use the already existing ones. Moreover, since the sensing device is located on the proximal end of the guide wire, no sensor is needed to be placed in direct contact with the patient organs. This will result in less complex than the existing solutions, which should allow a faster clinical approval.

In terms of comparison of performance for identify or classify a guide wire perforation event, unfortunately none of the aforementioned approaches focuses on perforation and they did not present quantitative results using a large number of experiments. This is why the performance of the proposed bispectral-based feature extraction algorithm can only be compared with the algorithm proposed by our research group in Refs. [21,22]. In Ref. [21] only 300 recordings have been used for evaluation and with a simple thresholding procedure over an indicator computed from different autoregressive (AR)-based features an accuracy of 89.5% for detecting perforation was obtained. For evaluation purposes in Ref. [22] the same database of this work was used and using 16 AR-based features and a SVM classifier an accuracy of 92% was obtained. The bispectral approach used in this work outperforms the results obtained in Ref. [22]. The four tested classification procedures obtained an accuracy between 97% and 98.73%. In terms of sensitivity and specificity also the new proposed bispectral approach obtain better results. In Ref. [22] the obtained specificity and sensitivity was 90.9%

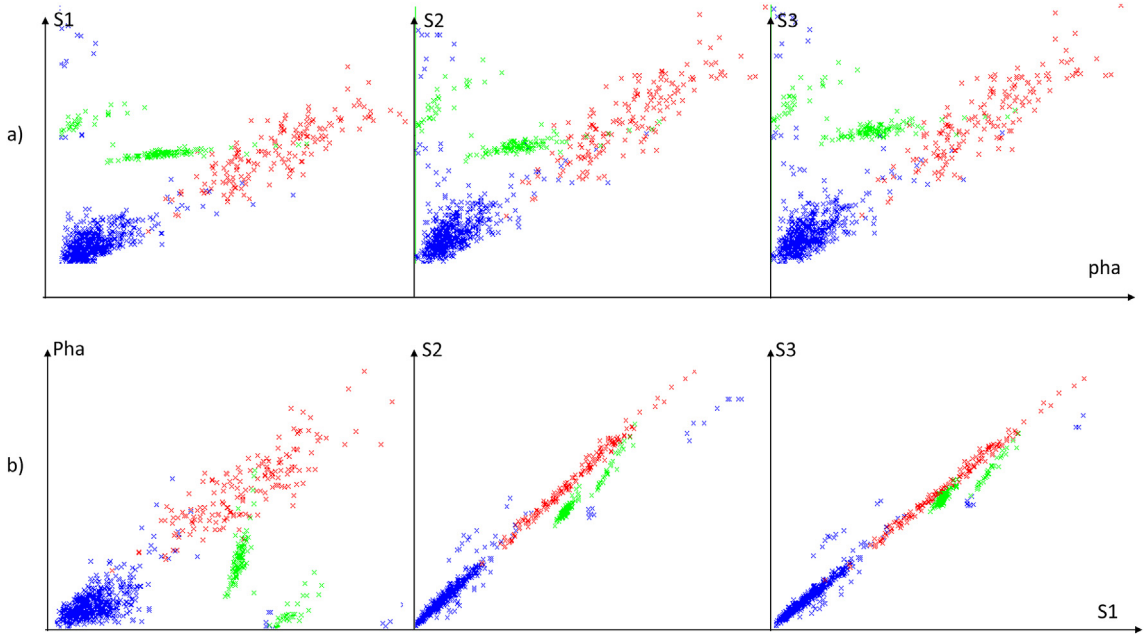

Fig. 8. 2D scatters between the four best ranked features.

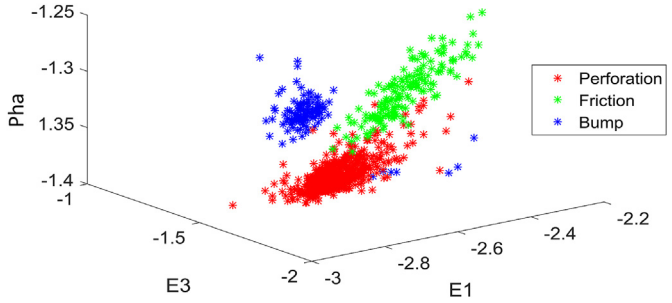

Fig. 9. 3D scatter for three selected features.

Table 2
Accuracy, sensitivity and specificity of the proposed approaches, K-NN, SVM-1 (polykernel), SVM-2 (RBF), and ANN. The True Positive (TP) and False positive (FP) for the classification of guide wire perforation, friction and bump are also displayed.

Events		Perforation	Friction	Bump	Accuracy	Sensitivity	Specificity
K-NN	TP	0.979	0.982	1	98.28%	98.00%	99.00%
	FP	0.010	0.016	0.001			
SVM-1	TP	0.964	0.963	1	97.00%	96.00%	98.00%
	FP	0.019	0.013	0.015			
SVM-2	TP	0.987	0.970	1	98.62%	98.00%	98.00%
	FP	0.016	0.008	0.001			
A-NN	TP	0.987	0.976	1	98.73	99.00%	99.00%
	FP	0.013	0.007	0.003			

and 95.3%, respectively. In this new approach the obtained specificity is between 98% and 99% and the sensitivity betwen 96% and 99%. These results show that the proposed features can better deal with the non-linearities resulting from the interaction of the tip and the vessel, that the AR based approach was not able to do.

5. Conclusion

In this work a new approach for processing acoustic emission signals for monitoring vessel perforation is presented. The main advantage of this approach is that it takes into consideration the strong non linear characteristics that a guide wire event can involve, resulting from the dynamic interaction between the distal tip and the vessel wall.

The main technological issue of this paper was to answer the question if it is possible, under controlled ideal conditions, to obtain a signature or trace from the acquired audio signals that could be used for 1) recognizing or characterizing the dynamics of a guide wire perforation and being able to 2) distinguish perforation from other events present during a real clinical intervention. We showed that features estimated from a time-varying version of the bispectrum clearly can identify a perforation.

It is also possible to observe that the cloud of points generated by the relationship between features form three clear clusters belonging to each studied guide wire event, which shows the scientific validity of the results.

It is important to mention the limitations concerning clinical applicability, where other type of artifacts will be present and that additionally should be first real-time detected before the characterization. Certainly, the ideal laboratory conditions under how the experiments has been performed, where no other physiological noises are present (such us heart beat, breathing, peristaltic sound), are advantageous for our approach. This conditions allow the acquisition of audio signals where no artifact affects a perforation or friction sound and where a guide wire event can be easy to detect. However, since a perforation is characterized by a high concentration and release of energy just before and just after the guide wire tip crosses the vessel wall, we can assume that this high energy signature can be different from for example biological sound sources (as blood flow and heart beats) that are characterized by slower dynamical changes.

One important next step for making the presented processing approach more robust is in the estimation and tracking of the time-variant characteristics of a guide wire event. In this work the time-variant features were computed using a simple sliding window, where at each window the bispectrum was calculated. A future work is to characterize the time-variant characteristics of the bispectrum using better suited methods such as wavelet or empirical mode decomposition.

Acknowledgements

This research was financially supported by the Federal Ministry of Education and Research (BMBF) in the context of the INKA Project

(Grant Number 03IPT7100X).

References

[1] M.G. Gunning, I.L. Williams, D.E. Jewitt, A.M. Shah, R.J. Wainwright, M.R. Thomas, Coronary artery perforation during percutaneous intervention: incidence and outcome, Heart 88 (5) (2002) 495–498.

[2] A. Teis, E. Fernndez-Nofreras, O. Rodrguez-Leor, H. Tizn, N. Salvatella, V. Valle, J. Mauri, Coronary artery perforation by intracoronary guide wires: risk factors and clinical outcomes, Rev. Esp. Cardiol. 63 (06) (2010) 730–734.

[3] R. Guo, L. Yang, The successful use of autologous skin in management of guidewire induced distal coronary perforation, Clin. Case Rep. 5 (6) (2017) 1018–1021.

[4] C. Hatzfeld, T.A. Kern, Engineering Haptic Devices, Springer London Limited, 2016.

[5] T. Mei, T.A. Kern, S. Sindlinger, R. Werthschtzky, HapCath: highly miniaturized piezoresistive force sensors for interior palpation of vessels during angioplasty, World Congress on Medical Physics and Biomedical Engineering, September 7-12, 2009, Munich, Germany, Springer, Berlin, Heidelberg, 2009, pp. 228–231.

[6] T. Opitz, C. Neupert, T. Rossner, N. Stefanova, T. Meiss, R. Werthschtzky, Miniaturized Haptic User-Interface for Heart Catheterizations Concept and Design, Biomedical Engineering/Biomedizinische Technik, 2013.

[7] N. Stefanova, M. Hessinger, T. Opitz, R. Werthschtzky, Characteristic of a force sensing guide wire for minimally invasive cardiac surgery, Engineering in Medicine and Biology Society (EMBC), 2016 IEEE 38th Annual International Conference of the, IEEE, 2016, August, pp. 5220–5223.

[8] T. Opitz, Entwurf und Realisierung eines haptischen Assistenzsystems für Herzkatheteruntersuchungen, Doctoral dissertation, Technische Universitt (2016).

[9] B. Han, Y.J. Yoon, M. Hamidullah, A.T.H. Lin, W.T. Park, Silicon nanowire-based ring-shaped tri-axial force sensor for smart integration on guidewire, J. Micromech. Microeng. 24 (6) (2014) 065002.

[10] F. Ganet, M.Q. Le, J.F. Capsal, P. Lermusiaux, L. Petit, A. Millon, P.J. Cottinet, Development of a smart guide wire using an electrostrictive polymer: option for steerable orientation and force feedback, Sci. Rep. 5 (2015) 18593.

[11] M. Kern, Comparing ffr tools: new wires and a pressure micro-catheter, Cath. Lab. Dig. 24 (2016) 4–9.

[12] H. Sharei, R. Stoute, J.J. van den Dobbelsteen, M. Siebes, J. Dankelman, Data communication pathway for sensing guidewire at proximal side: a review, J. Med. Dev. 11 (2) (2017) 024501.

[13] A. Okamura, H. Ito, K. Iwakura, S. Kawano, K. Inoue, Y. Maekawa, ... K. Fujii, Detection of embolic particles with the Doppler guide wire during coronary intervention in patients with acute myocardial infarction: efficacy of distal protection device, J. Am. Coll. Cardiol. 45 (2) (2005) 212–215.

[14] M. Ferrari, G.S. Werner, P. Bahrmann, B.M. Richartz, H.R. Figulla, Turbulent flow as a cause for underestimating coronary flow reserve measured by Doppler guide wire, Cardiovasc. Ultrasound 4 (1) (2006) 14.

[15] M. Ahmed, E.A. Oliver, J. Puleo, C.D. Ingman, B.D. Walker, Combination Sensor Guidewire and Methods of Use. U.S. Patent No. 8,277,386, U.S. Patent and Trademark Office, Washington, DC, 2012.

[16] R. Stoute, M.C. Louwerse, V.A. Henneken, R. Dekker, Intravascular Ultrasound at the tip of a guidewire: concept and first assembly steps, Procedia Eng. 168 (2016) 1563–1567.

[17] R. Ghaffari, S. Lee, J. Work, J.A. Wright Jr., L. Klinker, Catheter or Guidewire Device Including Flow Sensing and Use Thereof. U.S. Patent No. 9,295,842, U.S. Patent and Trademark Office, Washington, DC, 2016.

[18] A. van der Horst, Guidewire-mounted Thermal Sensors to Assess Coronary Hemodynamics, (2012).

[19] N. Meller, R. Sela, D. Seter, L. Sobe, Medical Device Guidewire with a Position Sensor. U.S. Patent Application No. 14/292, (2014), p. 088.

[20] J. Palushi, H.F. Salazar, G.G. Sema, I. Fang, E.F. Hakun, K.P. Muni, Navigation Guidewire with Shielded Sensor Coil. U.S. Patent Application No. 15/899,091, (2018).

[21] A. Illanes, A. Schaufler, I. Maldonado, A. Boese, M. Friebe, I.I. Katheter, Time-varying acoustic emission characterization for guidewire coronary artery perforation identification, Computing 44 (2017) 1.

[22] A. Illanes, A. Boese, I. Maldonado, A. Pashazadeh, A. Schaufler, N. Navab, M. Friebe, Novel clinical device tracking and tissue event characterization using proximally placed audio signal acquisition and processing, Sci. Rep. 8 (1) (2018) 12070.

[23] E.C. Orosco, N.M. Lopez, F. di Sciascio, Bispectrum-based features classification for myoelectric control, Biomed. Signal Process. Control 8 (2) (2013) 153–168.

[24] L. Huang, Q. Sun, J. Cheng, Y. Huang, Prediction of epileptic seizures using bispectrum analysis of electroencephalograms and artificial neural network, Engineering in Medicine and Biology Society, 2003. Proceedings of the 25th Annual International Conference of the IEEE, vol. 3, IEEE, 2003, September, pp. 2947–2949.

[25] G.R. Kiranmayi, V. Udayashankara, Neural network classifier for the detection of epilepsy, Circuits, Controls and Communications (CCUBE), 2013 International Conference on, IEEE, 2013, December, pp. 1–4.

[26] U.R. Acharya, E.C.P. Chua, K.C. Chua, L.C. Min, T. Tamura, Analysis and automatic identification of sleep stages using higher order spectra, Int. J. Neural Syst. 20 (06) (2010) 509–521.

[27] R.G. Garcia, G. Valenza, C.A. Tomaz, R. Barbieri, Instantaneous bispectral analysis of heartbeat dynamics for the assessment of major depression, Computing in Cardiology Conference (CinC), 2015, IEEE, 2015, September, pp. 781–784.

[28] R.J. Martis, U.R. Acharya, K.M. Mandana, A.K. Ray, C. Chakraborty, Cardiac decision making using higher order spectra, Biomed. Signal Process. Control 8 (2) (2013) 193–203.

[29] N. Sezgin, The effect of obstructive sleep apnea on the electrocardiogram signals, 3rd International Symposium on Innovative Technologies in Engineering and Science, 2015, pp. 1300–1307.

[30] M. Nasrolahzadeh, Z. Mohammadpoory, J. Haddadnia, Higher-order spectral analysis of spontaneous speech signals in Alzheimers disease, Cognit. Neurodynamics 12 (6) (2018) 583–596.

[31] M. Nasrolahzadeh, Z. Mohammadpoory, J. Haddadnia, A novel method for early diagnosis of Alzheimers disease based on higher-order spectral estimation of spontaneous speech signals, Cognit. Neurodynamics 10 (6) (2016) 495–503.

[32] P. Henriquez, J.B. Alonso, M.A. Ferrer, C.M. Travieso, Review of automatic fault diagnosis systems using audio and vibration signals, IEEE Trans. Syst. Man Cybern.: Systems 44 (5) (2014) 642–652.

[33] J.J.G. de la Rosa, R. Piotrkowski, J.E. Ruzzante, Higher order statistics and independent component analysis for spectral characterization of acoustic emission signals in steel pipes, IEEE Trans. Instrum. Meas. 56 (6) (2007) 2312–2321.

[34] J.M. Grriz, J. Ramrez, C.G. Puntonet, J.C. Segura, An efficient bispectrum phase entropy-based algorithm for VAD, Ninth International Conference on Spoken Language Processing, 2006.

[35] R.J. Martis, U.R. Acharya, H. Adeli, Current methods in electrocardiogram characterization, Comput. Biol. Med. 48 (2014) 133–149.

[36] W.A. Zgallai, Second-and third-order statistical characterization of non-linearity and non-gaussianity of adult and fetal ECG signals and noise, Practical Applications in Biomedical Engineering, InTech, 2013.

[37] I.I. Jouny, R.L. Moses, The bispectrum of complex signals: definitions and properties, IEEE Trans. Signal Process. 40 (11) (1992) 2833–2836.

[38] J.C. Sigl, N.G. Chamoun, An introduction to bispectral analysis for the electroencephalogram, J. Clin. Monit. 10 (6) (1994) 392–404.

[39] M.E. Hossain, W.A. Jassim, M.S. Zilany, Reference-free assessment of speech intelligibility using bispectrum of an auditory neurogram, PLoS One 11 (3) (2016) e0150415.

[40] K.C. Chua, V. Chandran, U.R. Acharya, C.M. Lim, Higher order spectra based support vector machine for arrhythmia classification, 13th International Conference on Biomedical Engineering, Springer, Berlin, Heidelberg, 2009, pp. 231–234.

[41] B. Das, M. Talukdar, R. Sarma, S.M. Hazarika, Multiple feature extraction of electroencephalograph signal for motor imagery classification through bispectral analysis, Procedia Comput. Sci. 84 (2016) 192–197.

[42] T. Ghosh, T. Biswas, R. Khatun, A feature extraction scheme to classify motor imagery Movements Based on Bi-spectrum analysis of EEG, IOSR J. VLSI Signal Process. 6 (5) (2016) 28–35.

[43] R. Yuvaraj, M. Murugappan, N.M. Ibrahim, K. Sundaraj, M.I. Omar, K. Mohamad, R. Palaniappan, Detection of emotions in Parkinson's disease using higher order spectral features from brain's electrical activity, Biomed. Signal Process. Control 14 (2014) 108–116.

[44] D. Karimi, Spectral and Bispectral Analysis of Awake Breathing Sounds for Obstructive Sleep Apnea Diagnosis, (2013).

[45] E.B. Assi, L. Gagliano, S. Rihana, D.K. Nguyen, M. Sawan, Bispectrum features and multilayer perceptron classifier to enhance seizure prediction, Sci. Rep. 8 (1) (2018) 15491.

[46] U.R. Acharya, F. Molinari, S.V. Sree, S. Chattopadhyay, K.H. Ng, J.S. Suri, Automated diagnosis of epileptic EEG using entropies, Biomed. Signal Process. Control 7 (4) (2012) 401–408.

[47] S. Gne, K. Polat, . Yosunkaya, Efficient sleep stage recognition system based on EEG signal using k-means clustering based feature weighting, Expert Syst. Appl. 37 (12) (2010) 7922–7928.

[48] S. Chaplot, L.M. Patnaik, N.R. Jagannathan, Classification of magnetic resonance brain images using wavelets as input to support vector machine and neural network, Biomed. Signal Process. Control 1 (1) (2006) 86–92.

[49] C.W. Hsu, C.C. Chang, C.J. Lin, A Practical Guide to Support Vector Classification, (2003).

[50] M. Ring, B.M. Eskofier, An approximation of the Gaussian RBF kernel for efficient classification with SVMs, Pattern Recogn. Lett. 84 (2016) 107–113.

[51] J. Platt, Sequential Minimal Optimization: A Fast Algorithm for Training Support Vector Machines, (1998).

[52] M.F. Akay, Support vector machines combined with feature selection for breast cancer diagnosis, Expert Syst. Appl. 36 (2) (2009) 3240–3247.